



ELSEVIER

Available online at www.sciencedirect.com

SCIENCE @ DIRECT®

Optics Communications 225 (2003) 13–17

OPTICS
COMMUNICATIONS

www.elsevier.com/locate/optcom

Montgomery self-imaging effect using computer-generated diffractive optical elements

Jürgen Jahns^{a,*}, Hans Knuppertz^a, Adolf W. Lohmann^b

^a FernUniversität Hagen, Optische Nachrichtentechnik, Universitätsstr. 27/PRG, 58084 Hagen, Germany

^b Universität Erlangen-Nürnberg, Lehrstuhl für Nachrichtentechnik, Cauerstr. 7, 91058 Erlangen, Germany

Received 10 April 2003; received in revised form 16 July 2003; accepted 21 July 2003

Abstract

The Montgomery self-imaging phenomenon represents a generalization of the well-known Talbot effect. Here, it is implemented by using computer-generated diffractive optical elements. A Montgomery interferometer consisting of two phase-complementary elements is demonstrated and suggested as a device for temporal processing of optical signals in the ps/fs-regime.

© 2003 Elsevier B.V. All rights reserved.

PACS: 42.25.Bs; 42.40.Jv

Keywords: Diffraction; Optical information processing; Self-imaging; Talbot effect; Temporal processing

1. Introduction

Self-imaging of an optical wavefield, i.e., its replication in the longitudinal direction without the use of a lens is an interesting phenomenon for theoretical and experimental reasons. Well-known is the case of self-imaging for periodic objects first observed and described by Talbot [1]. Talbot self-imaging can be described in the following way: a (quasi-)monochromatic wavefield of wavelength λ with lateral period $1/v_1$ is also longitudinally periodic. The longitudinal period z_T – often referred

to as the Talbot-distance – is given as $z_T = 2/\lambda v_1^2$. The Talbot effect has been widely studied (see, for example, the articles by Winthrop and Worthington [2] and Patorski [3]) and used for a number of applications such as interferometry [4], imaging [5] and beam splitting [5–7]. Recently, we suggested the use of the Talbot interferometer for the processing of temporal signals [8].

Talbot self-imaging occurs for wavefields with lateral periodicity under the assumption of paraxial propagation. Montgomery [9] described a more general case and showed that lateral periodicity is a sufficient but not a necessary condition for self-imaging. According to Montgomery, self-imaging occurs for wavefields whose angular spectrum is confined to spatial frequencies that represent concentric rings of well-defined radii. An

* Corresponding author. Tel.: +492331987340; fax: +492331987352.

E-mail address: jahns@fernuni-hagen.de (J. Jahns).

exact formula for the radius ρ_n of the n th ring will be given in a later section, however, approximately it is $\rho_n \approx \sqrt{nv'}$. Such wavefields can be generated by 1- and 2-D objects. Furthermore, Montgomery self-imaging is not restricted to paraxial wavefields.

The Montgomery effect was independently studied by Lohmann [10] and Indebetouw [11,12]. In [12], we also find a first experimental demonstration. There it was suggested that a Montgomery wavefield could be generated either by a “diffracting mask” or by a virtual object using a Fabry–Perot etalon. The diffracting mask was implemented as a binary amplitude Fresnel zone plate which approximates the frequency spectrum required for Montgomery self-imaging. Previous attempts to applied Montgomery objects include [13] and [14]. In both cases, spatial filtering techniques were used. In [14], it is shown that – under suitable conditions – quasi-periodic and aperiodic ring pupils generate self-imaging wavefields. Here, a relationship to Bessel or “nondiffracting” beams [15] is of interest: each ring in the pupil is the source of a Bessel beam whose intensity distribution is invariant upon propagation. For Montgomery self-imaging to occur, the different Bessel beams, each characterized by a specific wave number, have to add up coherently at certain z -planes.

The earlier work just mentioned is based on analog experimental techniques and thus offers limited design flexibility. This situation can be improved by the use of computer-generated diffractive optical elements (DOEs). The design and fabrication of DOEs is well established nowadays [16]. Phase-only DOEs can be “custom-designed” for specific tasks by using iterative Fourier transform algorithms and fabricated by lithographic fabrication techniques. It is the goal of this paper to demonstrate this possibility for Montgomery self-imaging with the purpose to make this effect applicable in a similar way as the Talbot effect. For our demonstration experiments, we use an interferometer consisting of two DOEs, called “Montgomery interferometer” analogous to the Talbot interferometer [4] (Section 3). As a potential application and motivation for this work we describe in Section 4 the use of the Montgomery interferometer as an optical tapped delay-line for the pro-

cessing of temporal signals. We shall start, however, with a brief review of the self-imaging effect.

2. Theory of self-imaging

Here, we consider only the 1-D case. Generalization to two dimensions (in either cartesian or cylindrical coordinates) is straightforward. The “grating” is described as

$$G_1(x) = \int \tilde{G}_1(v) \exp(2\pi i vx) dv \quad (1)$$

with

$$\tilde{G}_1(v) = \sum_n A_n \delta(v - v_n). \quad (2)$$

Propagation from the G_1 -location over a finite distance Δz is described by

$$\tilde{G}_1(v) \rightarrow \tilde{G}_1(v) \exp \left[\frac{2\pi i \Delta z}{\lambda} \sqrt{1 - \lambda^2 v^2} \right]. \quad (3)$$

In the paraxial case, one may approximate this as

$$\tilde{G}_1(v) \rightarrow \tilde{G}_1(v) \exp[-i\pi \lambda \Delta z v^2]. \quad (4)$$

For this case, a linear grating with $v_n = nv_1$ (n : integer) yields the Talbot effect, i.e., self-images appear at locations $\Delta z = Mz_T = M(2/v_1^2 \lambda)$ with $M = 1, 2, 3, \dots$. Fractional Talbot images are observed for $\Delta z = (M/N)z_T$ where N is also an integer number.

Rather than asking the question, how the wavefield looks like that is generated by a periodic object, Montgomery [9] asked the question how an object has to look like in order to generate a wavefield with longitudinal periodicity. If a wavefield is z -periodic it must be representable in a Fourier series as

$$\begin{aligned} u(x, z) &= u(x, z + z_T) \\ &= \sum_m V_m(x) \exp(2\pi i m z / z_T). \end{aligned} \quad (5)$$

Inserting this expression into the Helmholtz equation yields a differential equation for the $V_m(x)$. Meaningful solutions result for spatial frequencies [9,10]

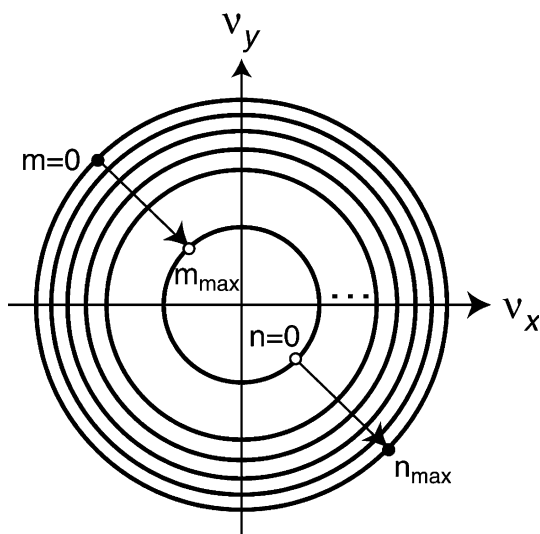


Fig. 1. 2-D spatial frequencies allowed for Montgomery objects according to Eq. (6). The little black dots mark the outermost frequency with index $m = 0$ or $n = m_{\max}$, respectively, whereas the little white dots mark the ring with index $n = 0$ or $m = m_{\max}$, respectively.

$$v_m^2 = \left(\frac{1}{\lambda}\right)^2 - \left(\frac{m}{z_T}\right)^2 \quad m = 0, 1, 2, 3, \dots, m_{\max}. \quad (6)$$

It should be noted that this result could have been also derived directly from Eq. (3) which represents a periodic function provided that Eq. (6) is valid.

For the 2-D case, we replace $v^2 \rightarrow v_x^2 + v_y^2$. In that case, the allowed frequencies for a Montgomery object represent concentric rings in the frequency plane (Fig. 1). Note, that the outermost ring with the highest spatial frequency occurs for $m = 0$. The maximum index, m_{\max} , occurs for the smallest spatial frequency and is given as the largest integer smaller than z_T/λ : $m_{\max} \leq z_T/\lambda$. Instead of m we may also use the index $n = m_{\max} - m$ which increases with the spatial frequency. For small values of n , one may write: $v_n \approx \sqrt{n}v'$ with $v' = v_{n=0}$ which is the paraxial limit to the Montgomery criterion [10]. In this case, one finds that $z_T \approx 2/\lambda v'^2$.

3. Experimental demonstration

In order to verify Montgomery self-imaging with DOEs, we use an experimental setup similar

to the Talbot interferometer [4]. It consists of two diffractive elements, G_1 and G_2 , separated by a multiple of the longitudinal period z_T (Fig. 2). For the experiments, G_1 and G_2 were implemented as phase-only computer-generated DOEs calculated by an iterative Fourier transform algorithm. Reminiscent of the rings occurring in the Montgomery theory, G_1 and G_2 were designed with a frequency spectrum consisting of seven rings as shown in Fig. 3(a). In order to keep fabrication and the experiment simple we chose the design parameters such that the spatial frequencies turned out to be relatively large. In our experiment, the longitudinal period was chosen to be $z_T = 10,000\lambda$ and $\lambda = 632.8$ nm. Each DOE consists of 513^2 pixels with a pixel size of $8 \times 8 (\mu\text{m})^2$ and four discrete phase levels (Fig. 3(b)). The far-field diffraction pattern of a single DOE is shown in Fig. 3(c). The diffraction efficiency was calculated to be 50.6%. This value is lower than typical values known for phase-only DOEs. We attribute this to the fact that in our demonstration experiment a wavefield with radial symmetry is generated by a DOE based on a cartesian grid. This mismatch leads to increased spatial quantization errors and thus to losses. It can be expected, however, that for other situations better optimization results and thus higher efficiencies can be achieved.

Self-imaging is now demonstrated by placing a second DOE at a distance z_T behind the first. We used two phase-complementary objects, i.e., $G_2 = G_1^*$, so that the wavefront behind G_2 should ideally be a plane wave that can be focused to a sharp spot in the Fourier plane. (This feature may

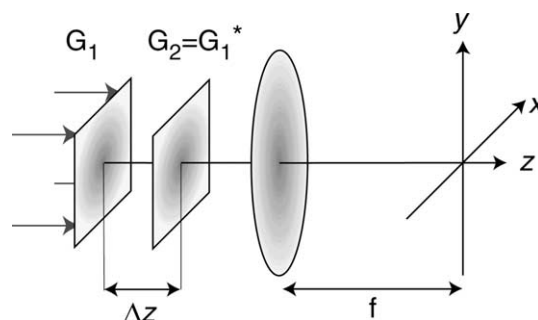


Fig. 2. Optical setup with two gratings at a distance Δz . The second grating is designed and positioned such that it is phase-complementary to the wavefield generated by G_1 .

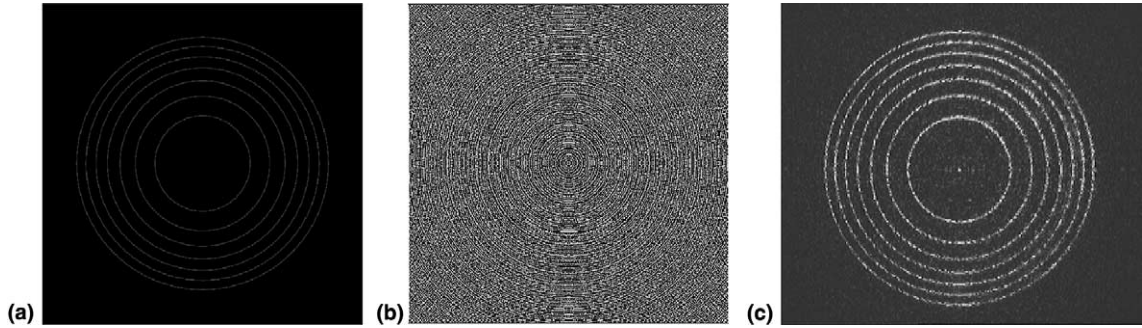


Fig. 3. (a) Designed diffraction pattern showing the rings in the Fourier plane according to Montgomery's theory. (b) Calculated phase grating consisting of 513^2 pixels, each grey level represents a different phase value. (c) Experimental diffraction pattern of the grating shown in (b).

eventually turn out to be useful to collect the light with a point detector.) As Fig. 4 shows, a sharp focal spot is indeed observed in the output plane as expected. Since each DOE generates unwanted diffraction orders and stray light as well, there is a certain amount of background illumination, which, however, is diluted over the output plane and, therefore, low in intensity. The efficiency of the interferometer was obtained by measuring the relative efficiency of the zeroth order. The measured value of approximately 19% was in close agreement with the calculated efficiency for the interferometer which is approximately 21%. The latter value is determined by the square of the efficiency of a single DOE (theoretical value approximately 25% in our case) and the reflection losses ($0.96^4 \approx 0.85$).

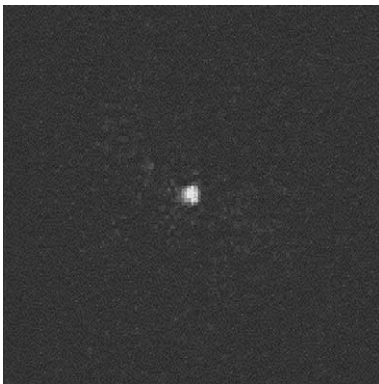


Fig. 4. Experimental diffraction pattern of two-grating setup as shown in Fig. 2. The DOEs were the same as those used for Fig. 3 separated by z_T .

4. Montgomery interferometer as a tapped delay-line filter

In [8], the Talbot interferometer was suggested for implementing a temporal tapped-delay line filter. As explained there, the temporal impulse response of the Talbot setup consists of a series of delayed delta-like impulses. Different group time delays result for different diffraction orders. More general, the temporal impulse response of an optical system is directly associated with its angular spectrum expressed in terms of the spatial frequencies v_x and v_y . The group time delay τ of a wave packet propagating under an angle α relative to the optical axis (here the z -axis) from a plane z to another plane $z + \Delta z$ is

$$\tau(\alpha) = \frac{\Delta z / \cos(\alpha)}{c}. \quad (7)$$

The directional cosine $\cos(\alpha) = \lambda v_z$ can be expressed by the spatial frequencies v_x and v_y to yield

$$\tau(v_x, v_y) = \frac{\Delta z}{c \sqrt{1 - \lambda^2 (v_x^2 + v_y^2)}}. \quad (8)$$

Consequently, any optical setup with an extended angular spectrum (1- or 2-D) has a temporal impulse response of finite extension and may, therefore, be potentially useful as a temporal filter.

The impulse response may be continuous or discrete. A discrete impulse response occurs, for example, when elements are used that generate a

discrete angular spectrum. The use of DOEs is of particular interest because of the design freedom they offer. Hence our interest in the Talbot and Montgomery interferometer as filtering devices. In the Talbot case, laterally periodic gratings are used which is equivalent to an equidistant spacing of spatial frequencies: $v_n = nv_1$. This choice of spatial frequencies, however, results in a quadratic increase of the time delay of the n th diffraction order

$$\begin{aligned}\tau_n(v_x) &= \frac{\Delta z}{c\sqrt{1 - (\lambda v_n)^2}} \\ &\approx (\Delta z/c)[1 + (1/2)(n\lambda v_1)^2].\end{aligned}\quad (9)$$

In the case of the Montgomery interferometer, however, the spatial frequencies are given by Eq. (6). Inserting this into Eq. (8) and using $\Delta z = M \cdot z_T$ we now obtain a time delay τ_m that increases linearly with the index m of the diffraction order

$$\tau_m = mM \frac{\lambda}{c}.\quad (10)$$

Note, that this is an exact result. Alternatively, we could have used the approximate, yet more intuitive, equation for the spatial frequencies of a Montgomery object consisting mostly of “coarse” structures for which $v_n \approx \sqrt{n}v'$. With this and by using the same approximation as in Eq. (9), we also arrive at the linear dependency between the time delay and the diffraction order.

To summarize the contents of this section: by going from linear gratings with equidistant spacing of the spatial frequencies as in the Talbot case to a Montgomery object with nonlinear (approximately square-root-like) spacing of the spatial frequencies, we can build an interferometric device that implements linear time shifts. This may be of interest to build a tapped-delay-line filter with applications for ps/fs-pulses. The use of computer generated diffractive elements allows one the flexible design of specific filter responses.

5. Conclusion

We have demonstrated Montgomery self-imaging with computer-generated diffractive optical elements. For the experimental demonstration, the Montgomery interferometer was used. The flexibility in the design of DOEs opens up the possibility to apply the Montgomery effect to different tasks in optical information processing, similar to the Talbot interferometer. As a specific example we suggest the use of the Montgomery interferometer as a temporal filter for Terahertz and optical frequencies. The use of 1-D “gratings” appears attractive for multiplexing purposes. More work is currently ongoing. This includes theoretical and experimental work on the temporal properties of the Montgomery interferometer and considerations on the potential and limitations for temporal signal processing as well as practical implementations.

References

- [1] H.F. Talbot, *Philos. Mag.* 9 (1836) 401.
- [2] J.T. Winthrop, C.R. Worthington, *J. Opt. Soc. Am.* 55 (1956) 373.
- [3] K. Paturski, *Progr. Opt.* 27 (1989) 1.
- [4] A.W. Lohmann, D.E. Silva, *Opt. Commun.* 2 (1971) 413.
- [5] O. Bryngdahl, *J. Opt. Soc. Am.* 63 (1973) 416.
- [6] R. Ulrich, T. Kamiya, *J. Opt. Soc. Am.* 68 (1978) 583.
- [7] A.W. Lohmann, *Optik* 79 (1988) 41.
- [8] J. Jahns, E. ElJoudi, D. Hagedorn, S. Kinne, *Optik* 112 (2001) 295.
- [9] W.D. Montgomery, *J. Opt. Soc. Am.* 57 (1967) 772.
- [10] A.W. Lohmann, *Optical Information Processing*, Erlangen, 1978 (Chapter 18).
- [11] G. Indebetouw, *Opt. Acta* 30 (1983) 1463.
- [12] G. Indebetouw, *Opt. Acta* 35 (1988) 243.
- [13] J. Ojeda-Castañeda, P. Andrés, E. Tepichin, *Opt. Lett.* 11 (1986) 551.
- [14] G. Indebetouw, *J. Opt. Soc. Am. A* 9 (1992) 549.
- [15] J. Durnin, *J. Opt. Soc. Am. A* 4 (1987) 651.
- [16] S. Sinzinger, J. Jahns, *Microoptics*, second ed., Wiley-VCH, Weinheim, 2003.